

# Electron Effective Mass of GaAs Double-Concentric Quantum Rings

I. Filikhin\*, E. Deyneka\*\* and B. Vlahovic\*

\*Physics Department, North Carolina Central University, 1801 Fayetteville St.

Durham, NC 27707, USA, Physics@nccu.edu;

\*\* Cree Inc, 4600 Silicon Drive, Durham, NC 27703

## ABSTRACT

We carried out the calculations for the single carrier energy levels, and the optical transitions of these structures, with taking into account the effects resulting in change of the electron effective mass due to the GaAs/Al<sub>0.3</sub>Ga<sub>0.7</sub>As quantum ring (QR) and concentric double quantum rings (DQR) geometry transformation. We applied a single sub-band 3D model for GaAs QD/QR with the energy dependence of the electron effective mass. Our prediction for the electron effective mass of the DQR ground state is 0.077m<sub>0</sub>, which is 13% greater than the bulk value of 0.067m<sub>0</sub>. The effects of small variations of the geometrical profile on the electron energies of the quantum structures were also studied.

**Keywords:** quantum rings, single electron levels, optical properties

## 1 INTRODUCTION

Successful fabrication of nano-sized self-assembled quantum dots (QD) and quantum rings (QR) with controlled geometrical properties has emphasized their potential for practical photonic device applications. Currently a well-established process of QD formation by the epitaxial growth and consecutive transformation of the QD into the QR [1, 2] paves the way to production of various 3D structures. Recent experiments reported in [3, 4] described two structures (GaAs/Al<sub>0.3</sub>Ga<sub>0.7</sub>As) made sequentially: GaAs quantum rings with the diameter of 40 nm, and the height of 15 nm, and concentric double quantum rings (DQR) consisted of the inner ring of the diameter of 40 nm and the height of 6 nm, and the outer ring of the diameter of 80 nm and the height of 5 nm. A theoretical analysis based on a single sub-band kp-theory for unstrained quantum nano-sized structures demonstrated quite a good agreement with the far-field PL spectrum measurements [4] for the first two excitations ( $N = 0, 1$ ).

In opposite for this work we carried out the calculations for the single carrier energy levels, and the optical transitions of these structures, with taking into account the effects resulting in change of the electron effective mass due to the QR/DQR geometry transformation. For the calculations a single sub-band 3D model for GaAs QD/QR with the energy dependence of the

electron effective mass [5-10] was applied. Our prediction for the electron effective mass of the DQR ground state is 0.077m<sub>0</sub>, which is 13% greater than the bulk value of 0.067m<sub>0</sub>. The contribution of the non-parabolic effect to the energy levels was evaluated. The effects of small variations of the geometrical profile on the electron energies of the quantum structures were also studied.

## 2 FORMULATION

Quantum nanosizes object (QD or QR) having cylindrical symmetry is embedded into the substrate. The discontinuity of the conduction band edge of the QD/QR and the substrate forms a band gap potential, which induces confinement carrier states. Using the single subband approach, this problem can be devised in the form of the Schrödinger equation:

$$(H_{kp} + V_c(\mathbf{r}))\Psi(\mathbf{r}) = E\Psi(\mathbf{r}). \quad (1)$$

Here  $H_{kp}$  is the one band kp Hamiltonian operator  $H_{kp} = -\nabla \frac{\hbar^2}{2m^*(E, \mathbf{r})} \nabla$ ,  $m^*(E, \mathbf{r})$  is the carrier effective mass, and  $V_c(r)$  is the band gap potential.  $V_c(r) = 0$  inside the QD (QR) and it is equal to  $E_c$  outside of the QD (QR), where  $E_c$  is defined by the conduction (or valence) band offset  $E_c = \kappa(E_g^{Sub.} - E_g^{QD})$ . Here  $\kappa$  is coefficient less 1 and can be different for conductor and valence bands. In order to account for the non-parabolic effect, the energy dependence of the electron effective mass is introduced:

$$m^*/m_0 = f(E, \mathbf{r}), \quad (2)$$

where  $m_0$  is the free electron mass, and  $f(E, \mathbf{r})$  is a function of the confinement energy [6, 7]. The non-linear Schrödinger equation (1) can be solved by the iteration procedure [7, 8]. In each step of the iterations the equation (1) is reduced to a linear Schrödinger equation, which is solved numerically by the finite elements method in cylindrical coordinates  $(\rho, z)$ . The carrier energy states in considered QD (QR) are classified by the radial  $n = 0, 1, 2, \dots$  and orbital  $l = 0, \pm 1, \pm 2, \dots$  quantum

numbers. The details of the formalism and the numerical procedure can be found in [9].

### 3 NUMERICAL SIMULATIONS

GaAs/Al<sub>0.3</sub>Ga<sub>0.7</sub>As QRs and DQRs rings, embedded into the AlGaAs substrate, were considered. Utilizing a droplet-epitaxial technique, Kuroda et al. [3, 4] recently were able to create nanometer-sized quantum ring complexes, consisting of a well-defined inner ring and the outer ring (DQR). The observed optical spectra [4] were interpreted on the basis of single carrier effective mass calculations. This consideration was restricted by the electron end heavy hole carriers, and the Coulomb interaction was excluded.

Let's point out here to the *geometry variation aspects* in the theoretical description of these GaAs/AlGaAs structures. The geometry effect can be described quite well by the recalculations within the framework of the simple model above, using the same input parameters, the effective masses of the carriers, and the confinement potentials, as in [4]:  $m_{GaAs}^*/m_{AlGaAs}^*=0.067/0.093$ ,  $E_c=183$  meV for the electron, and  $m_{GaAs}^*/m_{AlGaAs}^*=0.51/0.57$ ,  $E_c=137$  meV the for heavy hole. Since a profile of the quantum dots in [4] was not explicitly given, the values of the height, the outer, and interior radii, listed in [4], were used, along with the QR profile being close to the one presented in [3] (see figure 1 b-c)). The calculations for the electron and heavy hole energy levels of the QR are presented in figure 1.

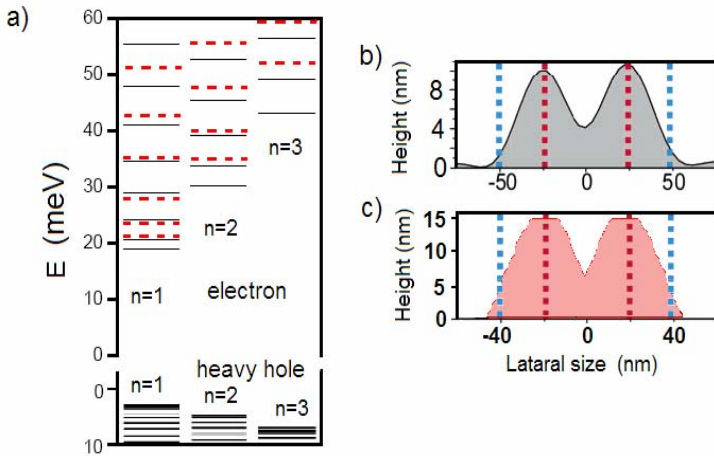


Figure 1 a) Single-carrier energy levels in QR. The solid lines correspond to the calculations of [4]. The radial quantum number  $n$  of the levels and the corresponding various quantum orbital numbers  $l = 0, 1, 2, \dots$  are shown. b) A cross-section of the QR obtained by microscopic measurements and reported in [3]. c) A cross-section of QR used in our calculation.

One can see that QR profile variation leads to a notable difference in the electron energies. Our calculation for the heavy hole shows a result similar to [4], due to a large value of the effective mass. The calculations of [4] were then compared with the experimental data obtained from the PL spectra. Geometrical uncertainty, however, does not allow for an accurate comparison between the calculations and the experimental data. In figure 2 the calculated optical transition energies of QR are shown with the experimental result from [4].

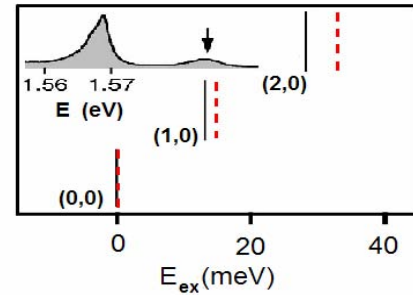


Figure 2. Calculated optical transition energies in QR. The results obtained by our calculations are shown by the dashed lines. The solid lines correspond to the [4]. The observed PL spectrum of QR [4] is shown in the inset.

One can notice the essential difference between our calculations and the ones of Kuroda et al, in particular, for the (0,0)-(0,2) transition. Taking the errors of the QR fabrication process into account, we can conclude that the sensitivity of the third excited state to the QR profile makes the observation of the transmission difficult. To explain the observed difference we have to consider variations in the energy characteristics of carriers due to quantum ring geometry. The energy dependence of the electron ground state of a simple symmetric shape can be derived according to [9, 10]:

$$E \cong a \left( \frac{1}{\Delta R} \right)^\gamma + b \left( \frac{1}{H} \right)^\beta, \quad (3)$$

where  $a$  and  $b$  are the coefficients weakly depending on geometry. The values of the power constants  $\gamma=1$  and  $\beta=1/3$  were obtained numerically by the mean square method for the ellipsoidal shape quantum ring [10]. Obviously, in the case of a potential well with infinite walls the relation (3) will produce  $a=b=\pi^2 \hbar^2 / 2m^*$ , and  $\gamma=\beta=2$ . For more topologically complex quantum

objects a relation analogous to (3) will have the mixed term  $\left( \frac{1}{\Delta R} \right)^{\gamma_1} \left( \frac{1}{H} \right)^{\beta_1}$  among other members associated with geometrical parameters. It is clear, however, that the terms featuring an inverse proportionality to the geometric parameters will contribute the most to the energy. Thus, small variations of geometry of the nanosize objects

$(\Delta H, \Delta(\Delta R))$  will result in large partial derivatives and therefore produce relatively large contributions to the energy change:

$\Delta E = (\partial E / \partial H) \Delta H + (\partial E / \partial(\Delta R)) \Delta(\Delta R)$ . Since in a simple model with the infinite walls the energy depends on the quantum number  $n$  as  $E_n \sim n^2$ , it is clear that the increase in quantum number  $n$  of states will be accompanied by increase in the sensitivity of the electron energy to geometry variations for any arbitrary quantum ring.

To continue the study of the geometry effects in GaAs quantum rings, we considered two QRs with a small difference in the profile. The results of the calculation are shown in figure 3a). The corresponding profiles of QR are depicted in figure 3 b)-c). The results agree with the presented explanation for geometrical sensitivity of the energy of QR. In particular, the difference in the energies for the (2,0) state is greater than for the (1,0) state.

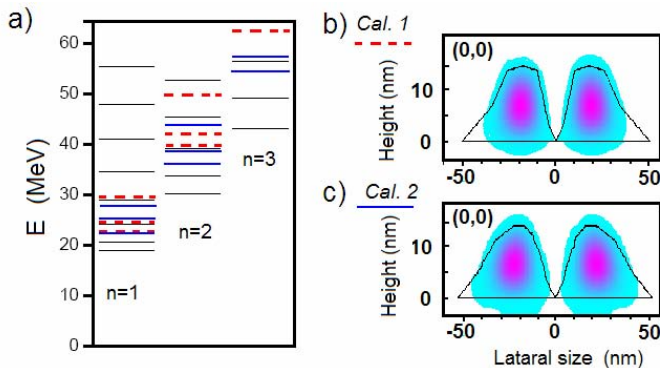


Figure 3. a) Single electron energy levels calculated for the various GaAs quantum rings profiles. The fine solid lines correspond to the calculations [4]. Our calculations are shown by the solid and dashed lines corresponding to the QR profiles depicted in figures 3 b) and 3c), respectively. The radial quantum numbers  $n$  of the levels and the corresponding quantum orbital numbers  $l = 0, 1, 2, \dots$  are shown. b)-c) Cross-sections of the QR used in our calculations. A counter plot of the electronic probability density in QR for the ground state is shown.

The double quantum ring (DOR) fabricated in [3, 4] is an example of the structure with more complex geometry. We have recalculated the data presented in [4] with the profile for a DOR, similar to the one used by Kuroda, et al. The results of our calculations for the energies of single electron levels are depicted in figure 4a). For comparison, we have also shown the results of the original work of [4]. The profiles for DQR used in our calculations, and in [4] are shown in figure 4b)-c). There is a slight discrepancy between the calculations, which cannot be conclusively explained. In particular, the difference for (1,0) level of a

heavy hole is surprising because the geometry difference would have been negated by a large effective mass of the heavy hole. This difference is important because it leads to dissimilar results for the (0,0)-(1,0) optical transmission, for which a good agreement with the experiment was previously obtained in [4]. Our calculations reveal a shift of the transmission energy towards the larger values. In Figure 5 the calculated transmission energies are shown along with the experimental data. Perhaps in this case we have an effect of the covered geometry factors for each ring of the DQR complex.

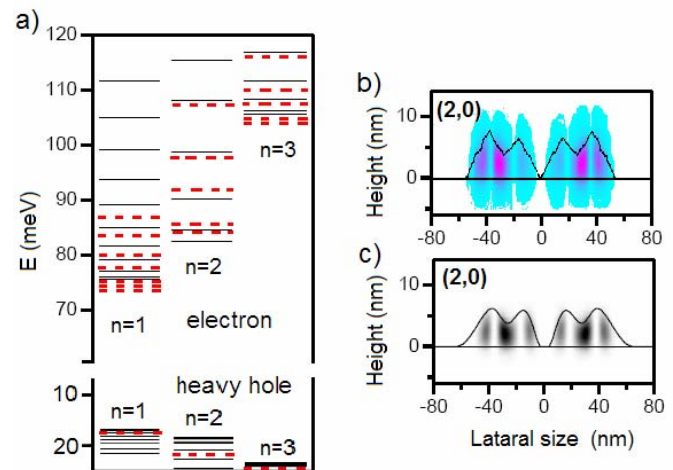


Figure 4. a) Single-carrier energy levels in DQR. The solid lines correspond to the calculations [4]. The radial quantum numbers  $n$  of the levels and the corresponding various quantum orbital numbers  $l = 0, 1, 2, \dots$  are shown; b) A cross-section of DQR used in our calculation; c) A cross-section of DQR corresponding to calculations reported in [4]. Counter plots of the electronic probability density in DQR for the (2, 0) state calculated in presented work and in [4] are shown.

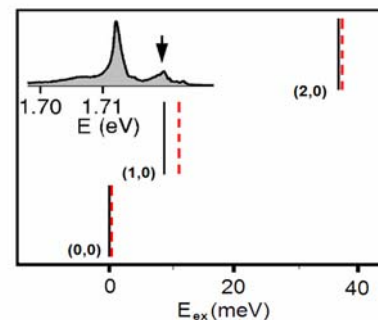


Figure 5. The calculated optical transition energies of DQR. Results, obtained by our calculations, are shown by dashed lines. The solid lines correspond to the results of [4]. The observed PL spectrum of DQR [4] is shown in the inset.

Another problem of interest related to the GaAs self-assembled structures deals with increase of the electron

effective mass of QD, QR and DQR, respectively. The non-parabolic effect leads to a change in the effective mass of the carriers in the quantum nanosize objects [2, 5].

The initial GaAs QDs are quite large in size; therefore for the QD this effect is minimal. The effective electron mass of the QD is practically equal to a bulk mass of the GaAs. At the present time the model of [4] was used, in which the electron effective mass was not subjected to change, therefore it was equal to a GaAs bulk mass. It should be noted that the fabrication of QRs and DQRs is accompanied by decreasing of the object size in one or two directions [4]. Taking the energy dependence of the electron effective mass into the account, we calculated the effective masses of the QR and DQR. The results of the calculations are shown in Figure 5, where a simple energy dependence of the effective mass (function  $f(\mathbf{r}, E)$  in (2)) is represented as a linear function connecting the points corresponding to the bulk values of the effective mass in GaAs and AlGaAs materials, respectively.

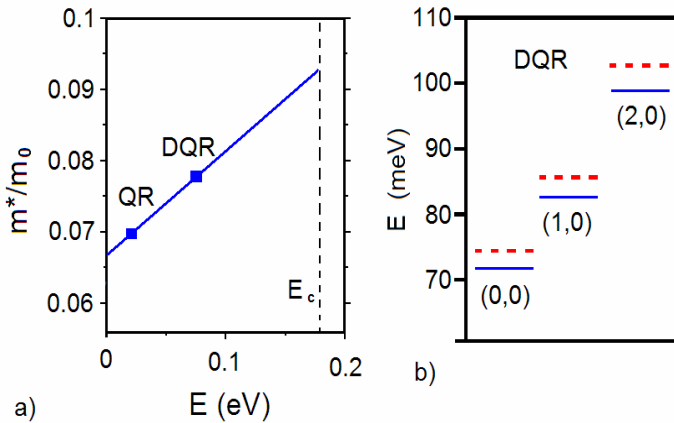


Figure 6 a) The energy of electron ground state and the GaAs electron effective mass. The solid line relates to the energy dependence of the effective mass used in calculations by the non-parabolic approximation. The line connects the points corresponding to the bulk values for GaAs and AlGaAs materials. The calculated values corresponding to QR (see Fig. 1c)) and DQR are marked by the squares. b) The energies of the first excited states of (DQR). The quantum numbers  $(n, l)$  of the states are shown. The calculations without taking into account the change in the electron effective mass due to non-parabolicity are shown by dashed lines. Solid lines correspond to the calculations in the framework of the non-parabolic approximation.

The apparent change in the effective mass is only existent for the DQR structure. Our prediction for the electron effective mass of the ground state is  $0.077 m_0$ , which is slightly larger (13%) than the bulk value of  $0.067 m_0$ . For the excited states the effective mass will have to increase to

the bulk value of the AlGaAs substrate. In Figure 6 the energy shifts of single electron levels due the non-parabolic effect are shown. One can see that the energies of the levels are shifted equidistantly, and this is a reason for the optical transmission spectrum in Figure 4 not to reveal any changes.

## 4 CONCLUSION

Nanosize quantum dots/quantum rings were studied in a single subband approach, with taking into account the non-parabolicity of the conduction band due to the energy dependence of the carrier effective mass. Realistic 3D geometry relevant to the experimental QD to QR fabrication was employed. The effects of small variations of the QD/QR geometrical shape parameters on the energy spectrum and the optical transmissions were calculated. By comparison with recent experimental and theoretical results, it is shown that the profile variations should be taken into the account for a correct interpretation of the experimental data. It is also shown that in modelling of self-assembled quantum objects, whose fabrication is accompanied by a decreasing size in at least one dimension, one has to take into account the non-parabolic effect, which, in turn, leads to a sufficient change in the electron effective mass.

This work was supported by the Department of Defense and NASA through Grants, W911NF-05-1-0502 and NAG3-804, respectively.

## REFERENCES

- [1] J. M. Garcia, G. Medeiros-Ribeiro, K. Schmidt, T. Ngo, and P. M. Petroff, Appl. Phys. Lett. 71, 2014-2016, 1997.
- [2] A. Lorke, R. J. Luyken, A. O. Govorov, and J. P. Kotthaus, J. M. Garcia and P. M. Petroff, Phys. Rev. Lett. 84, 2223-2226, 2000.
- [3] T. Mano, T. Kuroda, S. Sanguinetti, T. Ochiai, T. Tateno, J. Kim, T. Noda, M. Kawabe, K. Sakoda, G. Kido, N. Koguchi, Nano Letters 5, 425-4285, 2005.
- [4] T. Kuroda, T. Mano, T. Ochiai, S. Sanguinetti, K. Sakoda, G. Kido and N. Koguchi, Phys. Rev. B 72, 205301-8, 2005.
- [5] C. Wetzel, R. Winkler, M. Drechsler, B. K. Meyer, U. Rössler, J. Scriba, J. P. Kotthaus, V. Härle, F. Scholz, Phys. Rev. B 53, 1038-1050, 1996.
- [6] S. S. Li and J. B. Xia, J. Appl. Phys. 89, 3434, 2001.
- [7] Y. Li, O. Voskoboynikov, C. P Lee., S. M. Sze, O. Tretyak, J. Appl. Phys. 90, 6416-6420, 2002.
- [8] O. Voskoboynikov, Y. Li, H-M. Lu, C-F. Shih, C. P. Lee, Phys. Rev. B 66, 155306-155312, 2002.
- [9] I. Filikhin, E. Deyneka and B. Vlahovic, Mod. Simul. Mater. Sci. Eng. 12, 1121-1130, 2004.
- [10] I. Filikhin, E. Deyneka, H. Melikyan, and B. Vlahovic, Molecular Simulation 31, 779-785, 2005.